An improved kinetics approach to describe the physical stability of amorphous solid dispersions

Jiao Yang*, Kristin Grey, John Doney

ISP Pharma Technologies, 9176 Red Branch Rd., Suite R, Columbia, MD 21046, United States

ARTICLE INFO

ABSTRACT

The recrystallization of amorphous solid dispersions may lead to a loss in the dissolution rate, and consequently reduce bioavailability. The purpose of this work is to understand factors governing the recrystallization of amorphous drug–polymer solid dispersions, and develop a kinetics model capable of accurately predicting their physical stability. Recrystallization kinetics was measured using differential scanning calorimetry for initially amorphous efavirenz–polyvinylpyrrolidone solid dispersions stored at controlled temperature and relative humidity. The experimental measurements were fitted by a new kinetic model to estimate the recrystallization rate constant and microscopic geometry of crystal growth. The new kinetics model was used to illustrate the governing factors of amorphous solid dispersions stability. Temperature was found to affect efavirenz recrystallization in an Arrhenius manner, while recrystallization rate constant was shown to increase linearly with relative humidity. Polymer content tremendously inhibited the recrystallization process by increasing the crystallization activation energy and decreasing the equilibrium crystallinity. The new kinetic model was validated by the good agreement between model fits and experiment measurements. A small increase in polyvinylpyrrolidone resulted in substantial stability enhancements of efavirenz amorphous solid dispersion. The new established kinetics model provided more accurate predictions than the Avrami equation.

© 2009 Elsevier B.V. All rights reserved.

1. Introduction

The interest in amorphous drug–polymer solid dispersions has grown due to the potential of improving bioavailability, particularly for poorly water-soluble drugs (Leuner and Dressman, 2000; Craig, 2002; Hancock, 2002; Ahuja et al., 2007; Vippagunta et al., 2007). The basis for this interest stems from the increased rate of dissolution, which can range from hundreds- to thousands-fold increase, even for the most insoluble active pharmaceutical ingredients (APIs) (Leuner and Dressman, 2000). For drugs whose bioavailability is limited due to aqueous solubility (biopharmaceutical classification system BCS-2), the improved solubility may lead to enhanced bioavailability (Ambike et al., 2005; Khawam and Flanagan, 2006; Marsac et al., 2006a,b). The pharmaceutical potential of amorphous drug–polymer dispersions was realized with the nonnucleoside transcriptase inhibitor *Intelence* (etravirine) developed by Tibotec Pharmaceuticals, Ltd. Amorphous spray drying was credited with enhancing the bioavailability of this highly water-insoluble drug, increasing the plasma concentrations several orders of magnitude above the viral inhibitory concentration,

a feat that could not be accomplished with the crystalline form of the drug.

These advantages notwithstanding, advanced technologies often encounter challenges that must be understood and resolved in order to facilitate broad adoption. Amorphous solid dispersions face the perception that the amorphous form may not be thermodynamically stable (Ahlneck and Zografi, 1990; Yoshioka et al., 1994; Hancock et al., 1995, 1998) compared to the crystalline counterpart, and lead to unacceptable property changes. Most importantly, stable amorphous drug–polymer dispersion can be produced with proper formulation, enabling successful drug delivery. The goal of the current work is to understand the factors that can influence the recrystallization of amorphous drug–polymer solid dispersions, and develop a numerical model that accurately predicts the kinetics of recrystallization.

It is well known that APIs can be formulated with polymers to enhance their stability (Gupta and Bansal, 2004; Gupta et al., 2005; Konno and Taylor, 2006). The causal relationship between polymer addition and enhanced stability can be attributed to two mechanisms. First, long polymeric chain can sterically hinder the association among API molecules, and thus impede recrystallization. In addition, chemical interactions between the polymer and API tend to increase the energy barrier for nucleation, the initial event of recrystallization, and consequently enhance the physical

---

Nomenclature

API	active pharmaceutical ingredient
DSC	differential scanning calorimetry
EFV	efavirenz
J	nucleation rate
J_0	nucleation rate prefactor
k	recrystallization rate constant
k_0	prefactor of recrystallization rate constant
n	time exponent
PVP	polyvinylpyrrolidone
R	universal gas constant
RH	relative humidity
T_g	glass transition temperature
T_k	Kauzmann temperature
$V(t)$	crystalline volume
x_p	polymer ratio
$x(t)$	absolute crystallinity
x_∞	final absolute crystallinity
$\alpha(t)$	relative crystallinity
β	crystal growth rate
ΔE_A	activation energy
ΔH	melting enthalpy

stability. The amorphous drug–polymer dispersion is commonly characterized in terms of physical properties such as glass transition temperature (T_g), heat capacity, and miscibility (Clas et al., 1996; Hancock and Zografi, 1997; Marsac et al., 2006a,b; Wu and Yu, 2006). Though it is widely regarded that an increase in T_g indicates the improvement of physical stability, there is no direct evidence disclosed to relate T_g to recrystallization activation energy, the critical parameter evaluating stability. The entropy of supercooled liquid decreases rapidly on cooling toward glass transition temperature, T_g, and extrapolates to the entropy of crystal at so-called Kauzmann temperature, T_k (Kauzmqnn, 1948). The Kauzmann temperature (T_k), where molecular mobility is believed to be nil because of the extremely high viscosity (Ahlneck and Zografi, 1990; Yoshioka et al., 1994; Hancock et al., 1995, 1998; Kobayashi et al., 2000), has been recommended as an indicator of physical stability. However, it is a great challenge, or even impossible to increase T_k to typical storage temperature for drugs with considerably low melting points. Although factors governing physical stability still remain controversial and complicated, it is quite clear that the enhanced physical stability must be related to both the free energy of the amorphous materials relative to crystalline counterpart—the thermodynamic driving force for recrystallization, and factors which affect the kinetics of recrystallization, such as temperature, humidity and polymer carrier. Most of current approaches on stability prediction involve evaluation of T_g (Hodge, 1995; Moore et al., 1999; Corrigan et al., 2004; Miller and Lechuga-Ballersteros, 2006); however, T_g is not an intrinsic property and contingent to prior thermal history. Methods involving T_g measurement therefore are ambiguous. Hancock (1995) and Wu (2006) experimentally proved the surprising occurrence of nucleation below T_g, indicating that T_g is not a reliable indicator of physical stability. Methods based on either T_g or T_k are greatly compromised because they are incapable of physical stability quantification. Thus, it is of great interest to have a more reliable and accurate method for stability prediction, particularly for long-term conditions.

The objective of this study was to investigate the physical stability of initially amorphous drug–polymer solid dispersions based on recrystallization kinetics. The kinetics description comprises an approximation of the nucleation and crystal growth contribu-

tions, which are inherently essential to an accurate prediction. The kinetics approach offers direct and quantified evidence about the physical state for the studied materials, and grants the ability to estimate or even specify product shelf life without the time-consuming and costly long-term stability testing. Although the Avrami equation is commonly used to model crystallization kinetics for decades (Avrami, 1939, 1940), the reliability and accuracy is compromised because of its critical oversimplifications, most notably that the nucleation rate is constant throughout the recrystallization process. Other types of models also have been developed based on solid state reaction kinetics (Prout and Tompkins, 1944; Sheridan and Anwar, 1996; Supaphol and Spruiell, 2001; Wellen and Rabello, 2005; Yang et al., 2005a; Khawam and Flanagan, 2006; Ziaee and Supaphol, 2006), however there has been little progress in their applications to stability prediction of pharmaceutical solid dispersion.

In the present study, a new kinetics model was developed by correcting the critical oversimplification on nucleation rate in the Avrami equation (Avrami, 1939). The recrystallization kinetics was measured using DSC for amorphous dispersion containing efavirenz (EFV) and polyvinylpyrrolidone (PVP). In order to study the recrystallization kinetics, the polymer content levels were intentionally reduced below the level that produces stable, amorphous solid dispersions. These initially amorphous EFV–PVP solid dispersions were stressed with respect to elevated temperature and relative humidity (RH) so that the time frame for recrystallization occurred within an economically viable frame. Kinetics factors contributing to recrystallization rates were described in terms of activation energy under different storage conditions (temperature and RH) and formulation (PVP content). Finally, the model performance was examined and validated by comparing the model predictions with experiment measurements and predictions from the Avrami equation.

2. Materials and methods

2.1. Materials

Polyvinylpyrrolidone (Plasdone® K-29/32), was obtained from International Specialty Products Co., Wayne, NJ, USA, and efavirenz (chromatographic purity of 99.78%) was purchased from Aurobindo Pharma Ltd. (Hyderabad, India). Reagent grade methanol purchased from Sigma–Aldrich Co. (St. Louis, MO, USA).

2.2. Methods

2.2.1. Preparation of amorphous dispersion of efavirenz with PVP

Amorphous solid dispersions of EFV and PVP were prepared by spray drying technology. A series of compositions including EFV and PVP (Table 1) were dissolved in methanol to make a solution of 20% (w/w) total solids and visual observation of clear solution suggests the complete dissolving of the materials. 100 gram of the solution was spray dried under nitrogen environment using SD Micro™ spray dryer (Niro Inc., Columbia, MD, USA), and the powder product was collected at the product recovery cyclone. An inlet temperature of 70–75 °C, and outlet temperature of 40–45 °C, solution feed rate of 5 g/min, process pressure of 1.0 bar and atomization pressure of 1.5 bar were used during spray drying.

Table 1
Efavirenz-PVP solid dispersion compositions.

Ingredients	Compositions			
Efavirenz	83%	85%	84%	87%
PVP K-29/32	17%	15%	14%	13%

Table 2
The solid dispersion formulations and stability conditions for recrystallization kinetics study.

Composition of solid dispersion	Relative humidity	Temperature (°C)		
85% EFV:15% PVP	52%	67	70	72
Composition of solid dispersion	Temperature (°C)	Relative humidity (%)		
85% EFV:15% PVP	72	11	29	53
Relative humidity	Temperature (°C)	Composition (% efavirenz)		
53%	72	83	84	85	87

2.2.2. Differential scanning calorimetry (DSC)

A TA instrument Q1000^{TM} was used to determine the glass transition temperatures of the fresh made EFV solid dispersions with PVP and the melting enthalpy of those samples subject to stability conditions. Samples of 3–5 mg were analyzed using a heating rate of 20 °C/min from −40 °C to 180 °C. Crimped aluminium sample pan was used under a nitrogen purge at 50 mL/min. An empty pan was used as reference. Calibrations for temperature and enthalpy have been performed routinely with indium. Measurements were repeated three times.

2.2.3. Evaluation of crystallinity

The freshly spray dried powers were stored at stability chamber with temperature (±0.1 °C) and relative humidity (±1%) control (Table 2). Solid dispersion with 15% PVP was chosen to investigate the effect of temperature and relative humidity on the physical stability of amorphous efavirenz. Solid dispersion with 13%, 14%, 15% and 17% PVP were prepared and stored at 72 °C and 53% RH to investigate the effect of PVP on the physical stability of amorphous efavirenz solid dispersion. Samples were removed from storage at each time point and the extent of recrystallization was measured using DSC by heating the sample from −40 °C to 200 °C at 20 °C/min. The absolute percent crystallinity, $x(t)$, was determined as the ratio of melting enthalpies of recrystallized efavirenz over pure crystalline efavirenz (Avrami, 1941; Mao et al., 2006):

$$x(t) = \frac{\Delta H(t)}{\Delta H_m} \tag{1}$$

where $\Delta H(t)$ is melting enthalpy of recrystallized efavirenz at time t, which is calculated as the ratio of melting enthalpy of the sample divided by the composition of EFV and ΔH_m represents the melting enthalpy of 100% crystalline efavirenz at the same heating rate (Fig. 1).
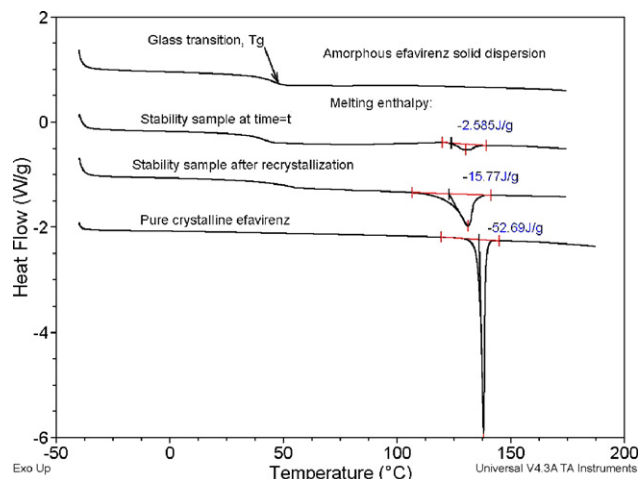
Fig. 1. Evaluating the fraction of recrystallized efavirenz using DSC.

An alternative expression for crystallinity used in the kinetics analyses is the relative crystallinity, $\alpha(t)$:

$$\alpha(t) = \frac{x(t)}{x(\infty)} = \frac{\Delta H(t)}{\Delta H_\infty} \tag{2}$$

where ΔH_∞ is the final melting enthalpy for the storage temperature and RH. The relative crystallinity, $\alpha(t)$, normalizes the true absolute crystallinity, $x(t)$, and varies from 0% to 100%.

2.2.4. Evaluation of recrystallization activation energy

An improved kinetics model was developed in order to quantify the physical stability of efavirenz amorphous dispersion. A nonlinear regression method (Pike, 1986) was applied to solve the model parameters based on the experimentally measured values of $\alpha(t)$.

2.2.5. Kinetics model

Recrystallization kinetics models have been proposed in the past decades to quantitatively describe the evolution of crystallinity (Avrami, 1939, 1940, 1941; Sheridan and Anwar, 1996; Supaphol and Spruiell, 2001; Wellen and Rabello, 2005; Yang et al., 2005b; Khawam and Flanagan, 2006; Ziaee and Supaphol, 2006). The Avrami model (Avrami, 1939, 1940, 1941) and Prout–Tompkins equation (Prout and Tompkins, 1944) are most frequently employed to describe solid state transformation kinetics. The Avrami model contains two essential assumptions: (1) the nucleation rate is constant with respect to time during recrystallization; and (2) crystal size grows linearly with respect to crystallization time from $t = 0$ to the final crystal size. In the Avrami model the relative crystallinity, $\alpha(t)$, is related to the crystallization time, t, according to the well-known Avrami equation:

$$\alpha(t) = 1 - \exp(-Kt^n) \tag{3}$$

where k represents crystallization rate constant and n is the Avrami exponent.

The crystallization rate constant, k, can be described in terms of activation energy, ΔE_A, and temperature, according to the Arrhenius rate law (Yoshioka et al., 1994):

$$k = k_o \exp\left(-\frac{\Delta E_A}{RT}\right) \tag{4}$$

where k_o is the pre-exponential factor, R is the universal gas constant and T is the absolute temperature in the unit of kelvin.

The assumptions of constant nucleation rate in the Avrami model described above lead to an overprediction in the recrystallization rate. Although the driving forcing for nucleation, the energy difference between amorphous state and crystalline state, remains constant at isothermal condition as crystallization proceeds, the nucleation rate, $J(t)$, tends to decrease with respect to time, because the available nucleation sites, the reactant, are consumed throughout the recrystallization process. In the present work an improved description of the nucleation rate is proposed that it is proportional to amorphous fraction, $1 - \alpha(t)$,

$$J(t) = J_o(1 - \alpha(t)) \tag{5}$$

where J_o is the initial nucleation rate and $1 - \alpha(t)$ is a function of crystallization time.

Nucleation is the initiation of crystallization and is followed by crystal growth (Oxtoby, 1992; Perez, 2005). Unlike nucleation, crystal growth exclusively depends on the thermodynamic driving force, the energy difference between amorphous state and crystalline state. It is widely accepted that crystals grow linearly with respect to crystallization time (Gutzow, 1977; Andronis and Zografi, 2000; Supaphol and Spruiell, 2001):

$$r = \beta t \qquad (6)$$

where r is the radius for spherical crystal and β is crystal growth rate. During the time interval τ to $\tau + d\tau$ the number of nuclei generated is:

$$N = J_0 (1 - \alpha(\tau)) d\tau \qquad (7)$$

Since each nuclei will grow into a sphere of radius $\beta(t - \tau)$ and so the increased volume due to nuclei appearing in the time interval will be:

$$dV(t) = \frac{4\pi}{3} \beta^3 (t - \tau)^3 J_o (1 - \alpha(\tau)) d\tau \qquad (8)$$

where $V(t)$ is the volume transformed into the crystalline state. It is also related to the relative crystallinity by the Avrami phase transition theory:

$$1 - \alpha(t) = \exp(-V(t)) \qquad (9)$$

The derivative of Eq. (9) provides an expression for the created crystalline volume in differential form:

$$dV(t) = \frac{1}{1 - \alpha(t)} d\alpha(t) \qquad (10)$$

A relationship between $\alpha(t)$ and t is established by solving Eqs. (8) and (10):

$$\frac{1}{[1 - \alpha(t)]^2} d\alpha(t) = \frac{4\pi}{3} \beta^3 J_0 (t - \tau)^3 d\tau \qquad (11)$$

Integration of above equation gives the final model equation for spherical crystal growth:

$$\alpha(t) = 1 - \frac{1}{1 + kt^4} \qquad (12)$$

where k is crystallization rate constant, expressed as the production of nucleation rate constant, J_o, and crystal growth rate constant, β, and retains the same physical meaning as in the Avrami equation:

$$k = \frac{1}{3} \pi \beta^3 J_o \qquad (13)$$

In Eq. (12), time is raised to the fourth power. A more general form for relative crystallinity can be presented as:

$$\alpha(t) = 1 - \frac{1}{1 + kt^n} \qquad (14)$$

where the exponent n describes the dimensionality of crystal growth, and equals 2, 3 and 4 for rod, plate, and spherical geometry, respectively for homogeneous nucleation (Table 3).

A general form of k can be expressed in terms of activation energy, ΔE_A, and T according to the Arrhenius rate law equation (4).
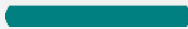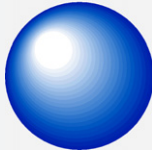
3. Results and discussion

3.1. Measurement of recrystallization kinetics of amorphous efavirenz using DSC

The fresh produced efavirenz solid dispersions samples were tested by DSC to verify the absence of initial crystallinity before

Table 3
Model parameters for one, two and three dimensional crystal growth (Avrami, 1939)[a] with homogenous nucleation.

Geometric structure	k	n
Rod	$A\beta J_o$	2
Plate	$2\pi\beta^2 h J_o$	3
Sphere	$1/3\pi\beta^3 J_o$	4

[a] A is the cross section surface area of the rod, and h is the thickness of the plat.

storage (Fig. 2). The absence of melting endotherm indicates the crystalline efavirenz was completely converted into amorphous form by spray drying. Samples after amorphous verification were then placed under stability storage condition immediately and were analyzed at a serial of time points. The occurrence of melting peak indicates the amorphous efavirenz transformed into crystalline form under the storage condition, and the integration value of the melting peak gives, according to Eqs. (1) and (2), the fraction of recrystallized efavirenz. Fig. 2 showed the recrystallization of amorphous efavirenz from solid dispersion with 15% PVP K-29/32 under stability storage condition of 72 °C and 11% relative humidity. The increasing magnitude of efavirenz melting peak indicates the proceeding of recrystallization.

3.2. Assessment of the new kinetic model

An initially amorphous solid dispersion containing 85% EFV:15% PVP began to recrystallize after 10 h of storage at 72 °C and 11% RH, and reached its final crystallinity after 9 days (Fig. 3). The char-
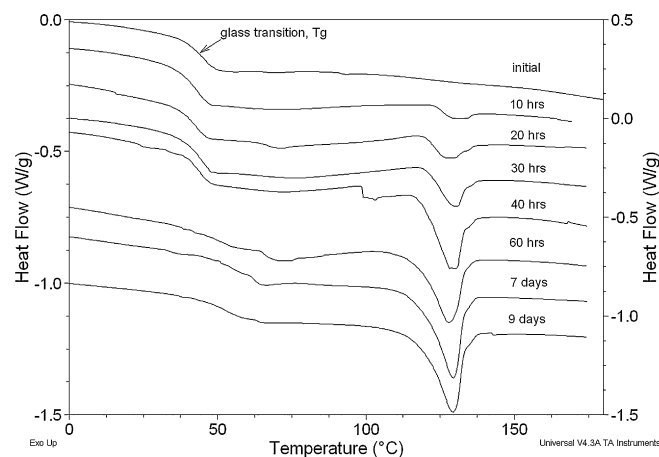
Fig. 2. The measurements of recrystallized efavirenz from solid dispersion with 15% PVP K-29/32 under 72 °C and 11% relative humidity by DSC at heating rate of 20 °C/min.
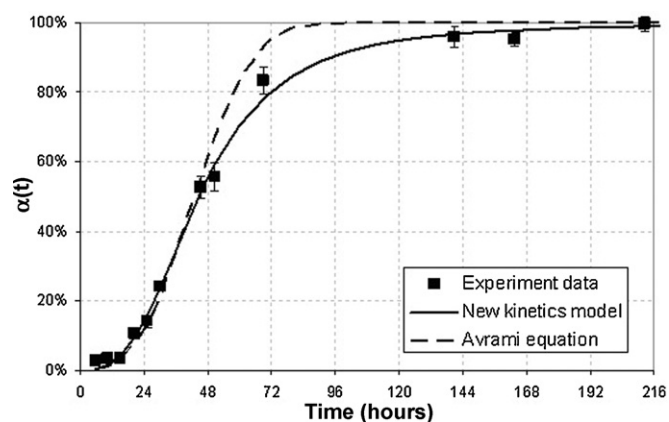
Fig. 3. Relative crystallinity, $\alpha(t)$, as a function of time for initially amorphous 85% EFV:15% PVP solid dispersion when stored at 72 °C and 11% RH. Error bar represents 1 standard deviation.
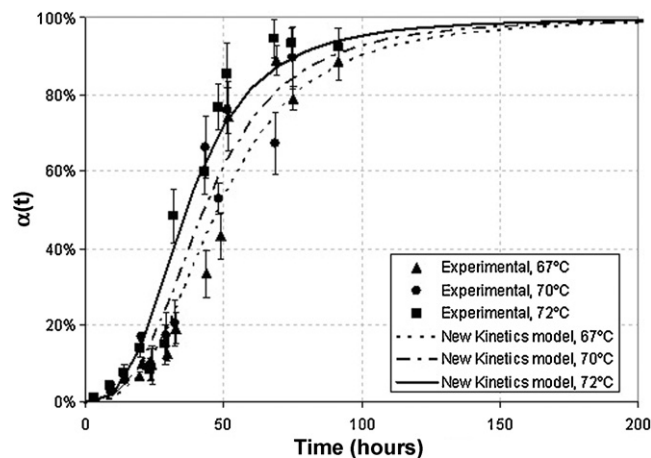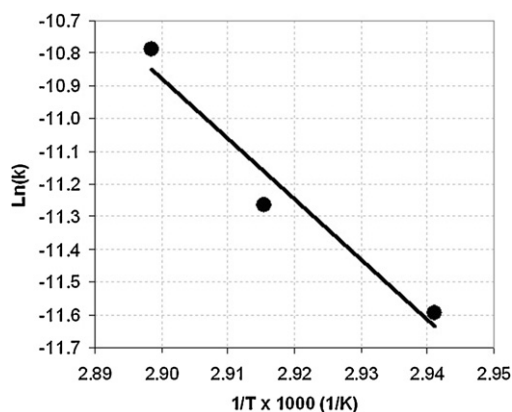

Fig. 4. Relative crystallinity, $\alpha(t)$, as a function of time for initially amorphous 85% EFV:15% PVP solid dispersion stored at 52% RH and 67 °C (▲), 70 °C (●) and 72 °C (■). Error bar represents 1 standard deviation.

acteristic "S" shape curve of recrystallization is due to the small number of nuclei at the very beginning, followed by a rapid recrystallization. Due to the consumption of nucleation sites, a decline in recrystallization rate was observed at late time of recrystallization.

Included with the experimental data in Fig. 3 are recrystallization predictions based on the Avrami model and the new kinetic model. The experiment measurements were fitted by the new model equation in comparison with the Avrami model by a multivariate nonlinear regression method (Pike, 1986). Initial values of $k = 0.1$ and $n = 1$ were given to compute the optimized values of model parameters by minimizing the sum of residual squares using successive linear programming method (MAP). Correlation coefficient, r^2, were tabulated in Table 4 and disclosed that the new model consistently provides better fit than the Avrami equation.

The Avrami equation (3) implicitly defines a constant nucleation rate, a simplification that overpredicts the relative crystallinity, $\alpha(t)$, and underpredicts the time for complete recrystallization. Only small deviations between the experimental data and the Avrami equation are noted during primary crystallization, because nucleation is approximately constant. However, during secondary (late-stage) crystallization, the nucleation rate decreases sharply due to the decline of available nucleation sites. For late-stage crystallization, a pronounced disagreement is observed between the experimental data and predictions from the Avrami equation. This disagreement has been occasionally reported (Gutzow, 1977; Hu et al., 2002; Perez, 2005; Wellen and Rabello, 2005). The simplified nucleation rate and resulting overprediction in $\alpha(t)$ elucidates the failure of the Avrami equation to accurately model secondary crystallization (Gutzow, 1977; Perez, 2005). This simplification was corrected in the new kinetic model, which proposes a linear relationship between nucleation rate and $\alpha(t)$. As seen in Fig. 3, the new kinetic model provides a more quantitatively accurate description of the experimental data for late-stage crystallization.

3.3. The effect of temperature on recrystallization rate constant

An initially amorphous solid dispersion containing 85% EFV:15% PVP was stored at three temperatures (67 °C, 70 °C, and 72 °C) and one RH (53%). The storage temperatures were selected to be higher than those normally used for pharmaceutical stability testing in order to promote recrystallization within a more economical time frame. Under all these conditions the characteristic S-shaped curve again was noted, with faster recrystallization at increasing temperature (Fig. 4). Using the nonlinear regression methods with the experimental data, k was estimated to be $9.3 \times 10^{-6}\,h^{-3}$, $1.21 \times 10^{-5}\,h^{-3}$ and $1.54 \times 10^{-4}\,h^{-3}$ for 67 °C, 70 °C and 72 °C, respectively. This 16.6-fold increase in k is noteworthy, especially given the 5 °C span in temperature. The estimated value of n is 3.0 for all three temperatures, indicating the same or similar nature of nucleation and crystal growth for all the three temperatures (Avrami, 1941).

The effect of temperature on recrystallization is also presented by the temperature dependence of recrystallization rate constant (Fig. 5). The semi-log plot of k vs $1/T$ reveals that the crystallization rate constant increased exponentially with temperature, T, within the temperature range studied (Hancock, 1960; Oxtoby, 1992; Supaphol and Spruiell, 2001), implying the Arrhenius equation correctly expresses the temperature dependence of recrystallization rate constant. The recrystallization activation energy, ΔE_A, was determined by the slope of the linear regression of $\ln k$ and $1/T$ (Corrigan et al., 2004). Solving of the activation energy allows the prediction of recrystallization kinetics at temperatures outside the experiment range.

Table 4
Model analysis of the recrystallization kinetics of efavirenz solid dispersion.

SDD formulation and stability condition	New kinetics model			Avrami model		
	n	$k \times 10^6$ (min^{-n})	r^2	n	$k \times 10^6$ (min^{-n})	r^2
15% PVP, 72 °C, 11%	3.0	9.92	0.994	3.0	6.43	0.987
15% PVP, 72 °C, 29%	3.0	85.2	0.976	3.0	39.2	0.956
15% PVP, 72 °C, 53%	3.0	154	0.965	3.0	91.3	0.952
15% PVP, 70 °C, 53%	3.0	12.1	0.971	3.0	7.7	0.966
15% PVP, 67 °C, 53%	3.0	9.26	0.976	3.0	5.94	0.974
14% PVP, 72 °C, 53%	3.0	13.5	0.984	3.0	6.23	0.97
13% PVP, 72 °C, 53%	3.0	39.0	0.968	3.0	14.3	0.96
17% PVP, 72 °C, 53%	3.0	8.75	0.997	3.0	2.15	0.973

Fig. 5. An Arrhenius plot of crystallization rate constant, k, as a function of temperature, T, for initially amorphous 85% EFV:15% PVP solid dispersion.

3.4. The effect of relative humidity on recrystallization rate constant

Initially amorphous 85% EFV:15% PVP solid dispersion was stored also at one temperature (72 °C) and three RH (11%, 29%, and 53%) to determine the influence of humidity on the recrystallization process. RH exerted great influence on recrystallization rate. Rapid recrystallization rates were observed under high relative humidity (Fig. 6). Using the nonlinear regression methods with the experimental data, k was estimated to be equal $9.92 \times 10^{-6}\,h^{-3}$, $8.52 \times 10^{-5}\,h^{-3}$, and $1.54 \times 10^{-4}\,h^{-3}$ for 11%, 29% and 53% RH respectively. The value of n was 3.0 for all the RH, again suggesting the same or similar nucleation and crystal growth mechanism.

Linear regression of the experimental data suggests that k increases linearly rather than exponentially over the range in RH studied (Fig. 7) (Ahlneck and Zografi, 1990). The increase of crystallization rate is attributed to the water-induced plasticization and ensuing enhanced molecular mobility (Hancock and Zografi, 1997; Marsac et al., 2006a,b).

### 3.5. The effect of PVP content on the stability of amorphous efavirenz

Four different amorphous efavirenz solid dispersions were produced to evaluate the effect of PVP level on the physical stability. These amorphous dispersions, containing 13%, 14%, 15%, and 17% PVP, were confirmed by DSC to be initially amorphous.
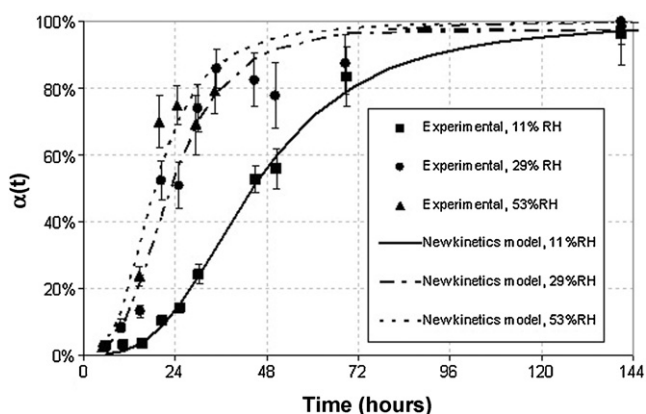
Fig. 6. Relative crystallinity, $\alpha(t)$, as a function of crystallization time for initially amorphous 85% EFV:15% PVP solid dispersion at 72 °C and 11% RH (■), 29% RH (●) and 52% RH (▲). Error bar represents 1 standard deviation.
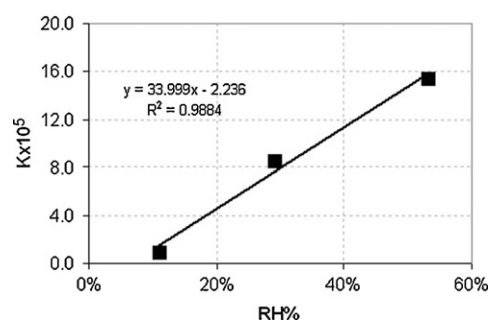
Fig. 7. Recrystallization rate constant as a function of relative humidity for initially amorphous 85% EFV:15% PVP solid dispersion.
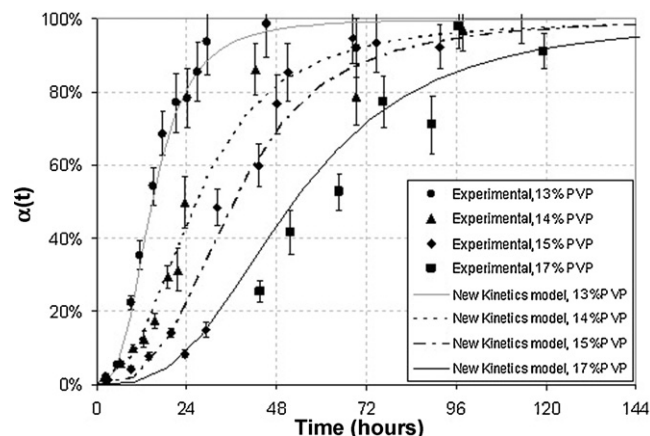
Fig. 8. Relative crystallinity, $\alpha(t)$, as a function of time for initially amorphous efavirenz–PVP solid dispersions containing 13% PVP (●), 14% PVP (▲), 15% PVP (♦), and 17% PVP (■) at 72 °C and 52% RH. Error bar represents 1 standard deviation.

Immediately after spray drying the three solid dispersions were stored at the same storage temperature (72 °C) and RH (53%). The experimental recrystallization data show a surprising decrease in recrystallization rate with increasing PVP content (Fig. 8). Using the nonlinear regression methods with the experimental data, k was estimated to be $3.90 \times 10^{-4}\,h^{-3}$, $1.35 \times 10^{-4}\,h^{-3}$, $1.54 \times 10^{-4}\,h^{-3}$ and $8.75 \times 10^{-6}\,h^{-3}$ for 13%, 14%, 15% and 17% PVP, respectively. This 45-fold decrease in k is remarkable, since the PVP content was changed only by 4%. Hence, PVP content is believed to be more influential in regulating efavirenz recrystallization more than temperature or RH. As before, the estimated values of the time exponent, n, are almost the same (3.0) and suggested no alteration of nucleation and crystal growth mechanism introduced by increasing the PVP content in the solid dispersion.

The inhibition in efavirenz crystallization by PVP in the amorphous solid dispersion is explained by the formation of glass solution (Hodge, 1995). The T_g of the amorphous dispersions increased 15 °C as the PVP content increased from 0% to 17%, supporting the hypothesis of efavirenz solubilization by PVP (Table 5). The linear relationship between $\ln(k)$ and PVP content (x_p), indicates that E_A increases linearly with respect to PVP content in the formulation (Fig. 9). Thus, crystallization rate constant increases exponentially with respect to polymer ratio in amorphous solid dispersions. Therefore, surprisingly more stable amorphous efavirenz

Table 5
T_g for efavirenz amorphous solid dispersions, measured using DSC at a 20 °C/min heat rate from −40 °C to 200 °C.

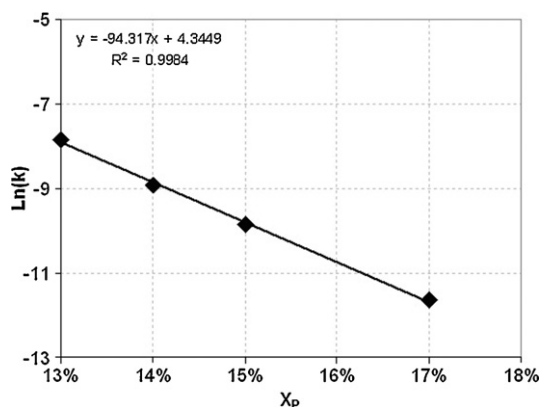| Weight percentage of Plasdone® K-29/32	0%	13%	14%	15%	17%	100%
T_g (°C)	33	51	45	46	48	174

Fig. 9. Logarithm plot of recrystallization rate constant as a function of PVP content for amorphous efavirenz solid dispersions stored at 72 °C and 52% RH.

solid dispersions can be made with small increases in PVP content in the formulation.

3.6. The effect of temperature, relative humidity and PVP ratio on the final extent of recrystallization

The actual extent of recrystallization, $x(t)$, can be calculated from experimentally measured values of enthalpy, *viz.*, Eq. (1). It is important to note that the initially amorphous efavirenz–PVP solid dispersions never fully recrystallize to produce 100% recrystallized drug regardless of the storage conditions. This experimental observation is attributed to the extremely high energy required for molecules trapped into polymer matrix to nucleate (Corrigan et al., 2004). For the studied formulations, it was impossible for all drug molecules to overcome the energy barrier and recrystallize. It was also surprising to note that the final extent of efavirenz recrystallization was measured to be relatively independent of temperature and relative humidity, although the recrystallization kinetics was found to be critically dependent on the storage condition (Figs. 4 and 6). The suspected reason is that efavirenz solubility in PVP solid solution is independent of temperature and relative humidity. Same amount of amorphous efavirenz will be converted into crystalline regardless storage temperature and relative humidity. In contrast, the final extent of efavirenz recrystallization decreases linearly with increasing PVP (Fig. 10). The increase of polymer ratio entraps more efavirenz molecules into the polymer matrix and reduces the final extent of recrystallization. The

intercept on polymer ratio axis gives the minimum amount of PVP required, 23.6%, to produce amorphous solid dispersion that will never recrystallize. This conclusion is also supported by our stability testing program for composition containing 75% EFV:25% PVP. We did not detect the occurrence of recrystallization after more than 24 months storage at 72 °C and 53% RH.

4. Conclusions

An improved kinetic model is presented that corrects the simplification in the Avrami equation. By considering the nucleation rate to be proportional to crystallinity, this new kinetic model more accurately describes efavirenz–PVP recrystallization than the Avrami equation, particularly for late-stage (secondary) crystallization. For early-stage formulation development of amorphous drugs, this approach can be especially valuable, as it saves the time and cost of conventional ICH stability testing. By solving of the relationships between recrystallization rate constant, temperature, relative humidity and formulation, an accurate and reliable prediction is obtained for recrystallization kinetics. Most significantly, the amount of polymer was found to be critical in promoting amorphous stability. The presence of PVP greatly inhibited not only the recrystallization process, but also reduced final extent of recrystallization, suggesting that enhanced stability can be achieved by increasing polymer level from formulation aspect.

References

Ahlneck, C., Zografi, G., 1990. The molecular basis of moisture on the physical and chemical stability of drugs in the solid state. Int. J. Pharm. 62, 87–95.
Ahuja, N., Katare, O.P., Singh, B., 2007. Studies on dissolution enhancement and mathematical modeling of drug release of a poorly water-soluble drug using water-soluble carriers. Eur. J. Pharm. Biopharm. 65, 26–38.
Ambike, A.A., Mahadik, K.T., Paradkar, A., 2005. Spray-dried amorphous solid dispersions of simvastatin, a low T_g drug: in vitro and in vivo evaluations. Pharm. Res. 22, 990–998.
Andronis, V., Zografi, G., 2000. Crystal nucleation and growth of indomethacin polymorphs from the amorphous state. J. Non-Cryst. Solids 271, 236–248.
Avrami, M., 1939. Kinetics of phase change I, general theory. J. Chem. Phys. 7, 1103–1114.
Avrami, M., 1940. Kinetics of phase change, II. Transformation-time relation for random distribution of nuclei. J. Chem. Phys. 8, 212–224.
Avrami, M., 1941. Granulation, phase change, and microstructure, kinetics of phase change. III, general theory. J. Chem. Phys. 9, 177–184.
Clas, S.D., Cotton, M., Moran, E., Spagnoli, S., Zografi, G., Vadas, E.B., 1996. Physical stability assessment of lyophilized MK-0591 by different scanning calorimetry. Thermochim. Acta. 288, 83–96.
Corrigan, D.O., Corrigan, O.I., Healy, A.M., 2004. Predicting the physical stability of spray dried composites: salbutamol sulphate/lactose and salbutamol sulphate/polyethylene glycol co-spray dried systems. Int. J. Pharm. 273, 171–182.
Craig, D.Q.M., 2002. The mechanism of drug release from solid dispersions in water-soluble polymers. Int. J. Pharm. 231, 131–144.
Gupta, P., Bansal, A.K., 2004. Molecular interactions in celecoxib-PVP-meglumine amorphous system. J. Pharm. Pharmacol. 57, 303–310.
Gupta, P., Thilagavathi, R., Chakraborti, A.K., Bansal, A.K., 2005. Role of molecular interactions in stability of Celecoxib-PVP amorphous systems. Mol. Pharm. 2, 374–391.
Gutzow, I., 1977. 1976 Crystal Growth and Material. North-holland, New York.
Hancock, B.C., 2002. Disordered drug delivery: destiny, dynamics and the Deborah number. J. Pharm. Pharmacol. 54, 737–746.
Hancock, B.C., Christensen, K., Shamblin, S.L., 1998. Estimation the critical molecular mobility temperature (T_k) of amorphous pharmaceuticals. Pharm. Res. 15, 1649–1651.
Hancock, B.C., Shamblin, S.L., Zografi, G., 1995. Molecular mobility of amorphous pharmaceutical solids below their glass transition temperature. Pharm. Res. 12, 709–806.
Hancock, B.C., Zografi, G., 1997. Characteristics and significance of the amorphous state in pharmaceutical systems. J. Pharm. Sci. 86, 1–12.
Hancock, H., 1960. Theory of Maxima and Minima. Dover Publication, Inc., New York.
Hodge, I.M., 1995. Physical aging in polymer glasses. Science 267, 1945–1947.
Hu, Y.S., Rogunova, M., Schiraldi, D.A., Hiltner, A., Baer, E., 2002. Crystallization kinetics and crystalline morphology of poly (ethylene naphthalate) and poly (ethylene terephthalate-co-bibenzoate). J. Appl. Polym. Sci. 86, 98–115.
Kauzmqnn, W., 1948. The nature of the glassy state and the behavior of liquid at low temperature. Chem. Rev. 43, 219–256.
Khawam, A., Flanagan, D., 2006. Solid-state kinetic model: basics and mathematical fundamentals. J. Phys. Chem. B 110, 17315–17328.
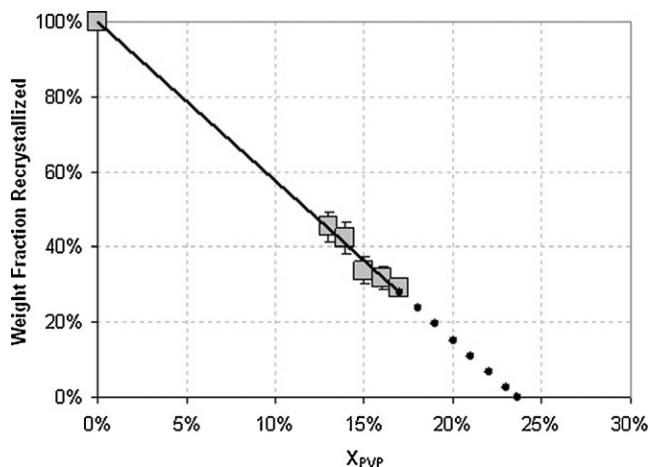
Fig. 10. The final efavirenz crystallinity as function of PVP content at 72 °C and 52% RH storage condition. Error bar represents 1 standard deviation.

Kobayashi, H., Takahashi, H., Hiki, Y., 2000. Viscosity of glasses near and below the glass transition temperature. J. Appl. Phys. 88, 3776–3778.

Konno, H., Taylor, L.S., 2006. Influence of different polymer on the crystallization tendency of molecularly dispersed amorphous felodipine. J. Pharm. Sci. 95, 2692–2705.

Leuner, C., Dressman, J., 2000. Improving drug solubility for oral delivery using solid dispersions. Eur. J. Pharm. Biopharm. 50, 47–60.

Mao, C., Chamarthy, S.P., Byrn, S.R., Pinal, R., 2006. A calorimetric method to estimate molecular mobility of amorphous solids at relatively low temperature. Pharm. Res. 23, 2269–2276.

Marsac, P.J., Konno, H., Taylor, L.S., 2006a. A comparison of the physical stability of amorphous felodipine and nifedipine systems. Pharm. Res. 23, 2306–2315.

Marsac, P.J., Shamblin, S.L., Taylor, L.S., 2006b. Theoretical and practical approaches for prediction of drug–polymer miscibility and solubility. Pharm. Res. 23, 2417–2426.

Miller, D.P., Lechuga-Ballersteros, D., 2006. Rapid assessment of the structure relaxation behavior of amorphous pharmaceutical solids: effect of residual water on molecular mobility. Pharm. Res. 23, 2291–2305.

Moore, G.V., Augustijns, P., Kinget, R., 1999. Stability prediction of amorphous benzodiazepines by calculation of the mean relaxation time constant using the Williams-Watts decay function. Eur. J. Pharm. Biopharam. 48, 43–48.

Oxtoby, D.W., 1992. Homogeneous nucleation: theory and experiment. J. Phys.: Condens. Matter 4, 7627.

Perez, M., 2005. Gibbs-Thomson effects in phase transformation. Scripta Mater. 52, 709.

Pike, R.W., 1986. Optimization for Engineering Systems. Van Nostrand Reinhold Company, New York.

Prout, E.G., Tompkins, F.C., 1944. The thermal decomposition of potassium permanganate. Trans. Faraday Soc. 40, 488–498.

Sheridan, A.K., Anwar, J., 1996. Kinetics of the solid-state phase transformation of form β to γ of sulfanilamide using time-resolved energy-dispersive X-ray diffraction. Chem. Mater. 8, 1042–1051.

Supaphol, P., Spruiell, J.E., 2001. Isothermal melt- and cold-crystallization kinetics and subsequent melting behavior in syndiotactic polypropylene: a differential scanning calorimetry study. Polymer 42, 699–712.

Vippagunta, S.R., Wang, Z., Hornung, S., Krill, S., 2007. Factors affecting the formation of eutectic solid dispersions and their dissolution behavior. J. Pharm. Sci. 96, 294–304.

Wellen, R.M.R., Rabello, M.S., 2005. The kinetics of isothermal cold crystallization and tensile properties of poly (ethylene terephthalate). J. Mater. Sci. 40, 6099–6104.

Wu, T., Yu, L., 2006. Surface crystallization of indomethacin below T_g. Pharm. Res. 23, 2350–2355.

Yang, J., McCoy, B.J., Madras, G., 2005a. Temperature effects for isothermal polymer crystallization. J. Chem. Phys. 122, 244905–244914.

Yang, J., McCoy, B.J., Madras, G., 2005b. Distribution kinetics of polymer crystallization and Avrami equation. J. Chem. Phys. 122, 64901–64911.

Yoshioka, M., Hancock, B.C., Zografi, G., 1994. Crystallization of indomethacin from amorphous state below and above its glass transition temperature. J. Pharm. sci. 83, 1700–1705.

Ziaee, Z., Supaphol, P., 2006. Non-isothermal melt- and cold-crystallization kinetics of poly (3-hydroxybutyrate). Polym. Testing 25, 807–818.